SCIENTIFIC REP{\Large O}RTS

OPEN

Switching of a large anomalous Hall effect between metamagnetic phases of a non-collinear antiferromagnet

Christoph Sürgers[1], Thomas Wolf[2], Peter Adelmann[2], Wolfram Kittler[1], Gerda Fischer[1] & Hilbert v. Löhneysen[1,2]

The anomalous Hall effect (AHE), which in long-range ordered ferromagnets appears as a voltage transverse to the current and usually is proportional to the magnetization, often is believed to be of negligible size in antiferromagnets due to their low uniform magnetization. However, recent experiments and theory have demonstrated that certain antiferromagnets with a non-collinear arrangement of magnetic moments exhibit a sizeable spontaneous AHE at zero field due to a non-vanishing Berry curvature arising from the quantum mechanical phase of the electron's wave functions. Here we show that antiferromagnetic Mn_5Si_3 single crystals exibit a large AHE which is strongly anisotropic and shows multiple transitions with sign changes at different magnetic fields due to field-induced rearrangements of the magnetic structure despite only tiny variations of the total magnetization. The presence of multiple non-collinear magnetic phases offers the unique possiblity to explore the details of the AHE and the sensitivity of the Hall effect on the details of the magnetic texture.

Among the magnetoelectronic transport phenomena, the Hall effect recently attracted renewed attention, in particular concerning antiferromagnetic materials[1–6]. The Hall effect generates a voltage V_x transverse to the current I_y in a perpendicular magnetic field H_z from which the Hall resistivity $\rho_{yx} = V_y t/I_x$ or the Hall conductivity $\sigma_{xy} \approx \rho_{yx}/\rho_{xx}^2$ are obtained (t: sample thickness along z direction, ρ_{xx}: longitudinal resistivity). In ferromagnets, the AHE ρ_{yx}^{AH}, i.e., the contribution in addition to the ordinary Hall effect $\rho_{yx}^0 = R_0 B$ caused by the Lorentz force acting on the charge carriers, appears as a consequence of broken time-reversal symmetry and spin-orbit coupling (SOC) and was suggested to depend linearly on the magnetization M, $\rho_{yx}^{AH} = R_S \mu_0 M$ or $\sigma_{xy}^{AH} = S_H M$[7]. However, even in materials with low or even zero magnetization, a geometrical or "topological" Hall effect arising solely from the electronic band structure independent of SOC is observed which is attributed to the non-vanishing Berry curvature of electrons migrating through a chiral spin texture[8–12]. The Berry curvature $\boldsymbol{\Omega}_n(\boldsymbol{k})$ of the nth band gives rise to an anomalous velocity $\boldsymbol{v}_n(\boldsymbol{k})$ of the Bloch electron in a given state $\boldsymbol{k}$ and a Hall current transverse to the electric field[8].

A large AHE has been predicted to occur also in antiferromagnets with a non-collinear arrangement of magnetic moments and zero spin-chirality, where SOC induces a Berry curvature and a sizeable AHE in zero magnetic field[5]. This has been recently proven for hexagonal Mn_3Ge[2] and Mn_3Sn[3], showing at room temperature spontaneous Hall conductivities of 50 and $30\,\Omega^{-1}\mathrm{cm}^{-1}$ in zero magnetic field, respectively. These values are of similar magnitude like in ferromagnetic metals and semiconductors. A large Hall response up to $200\,\Omega^{-1}\mathrm{cm}^{-1}$ has also been reported for the half-Heusler antiferromagnet GdPtBi originating from avoided crossings or Weyl points of the electronic band structure due to the breaking of time-reversal and lattice symmetry[1]. The results demonstrate that the large AHE of non-collinear antiferromagnets associated with low magnetization bears considerable potential for future applications. Thus, spintronic devices based on antiferromagnetic metals have been

[1]Physikalisches Institut, Karlsruhe Institute of Technology, P.O. Box 6980, 76049 Karlsruhe, Germany. [2]Institut für Festkörperphysik, Karlsruhe Institute of Technology, P.O. Box 3640, 76021 Karlsruhe, Germany. Correspondence and requests for materials should be addressed to C.S. (email: christoph.suergers@kit.edu).
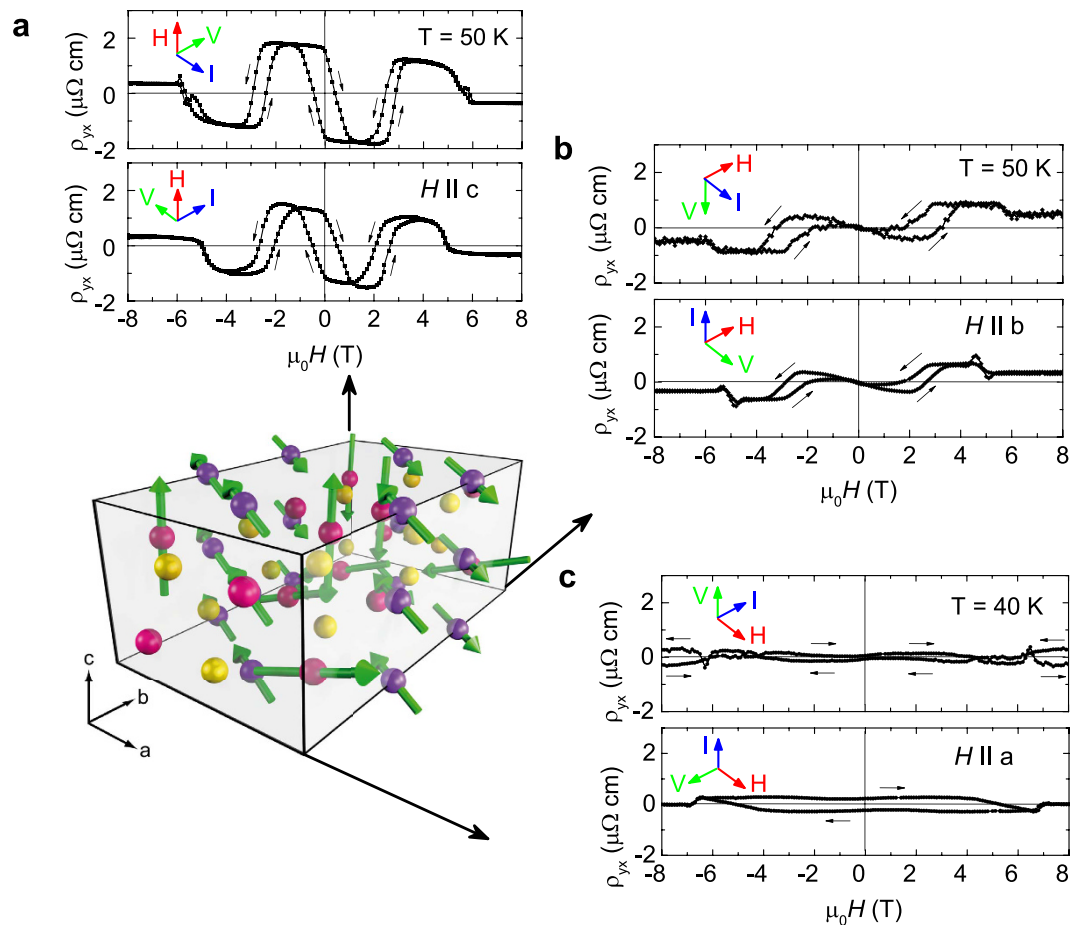
Figure 1. Anisotropic anomalous Hall effect of Mn$_5$Si$_3$. Schematic shows the non-collinear AF1 phase of Mn$_5$Si$_3$ below $T_{N1} = 60\,K$[19]. Solid lines delineate the orthorhombic unit cell. Green arrows visualize the magnetic Mn moments with their relative size indicated by the arrow length. (**a,b,c**) Hall resistivity for the magnetic field oriented parallel to the crystallographic c, b, and a axes of the orthorhombic structure, respectively.

proposed to show current-induced phenomena like in ferromagnets and new concepts for functional devices have been developed to exploit advantages specific to antiferromagnets[13–16].

Modifications of the AHE have been also observed for polycrystalline Mn$_5$Si$_3$ thin films in the non-collinear magnetic phase[17,18]. In contrast to Mn$_3$Ge[2] and Mn$_3$Sn[3], Mn$_5$Si$_3$ exhibits several different antiferromagnetic phases depending on magnetic field and temperature due to competing interactions between Mn moments. Below $T_{N2} = 100\,K$, the crystal structure has orthorhombic symmetry with two inequivalent Mn sites. The magnetic structure of this AF2 phase comprises a collinear arrangement of magnetic moments Mn$_2$. Below $T_{N1} \approx 60\,K$, the magnetic structure becomes highly non-collinear by realignment of Mn$_2$ moments, splitting into Mn$_{21}$ and Mn$_{22}$ moments, and additional ordering of Mn$_1$ moments due to a magneto-structural distortion (AF1 phase, Fig. 1)[19–22]. The three different Mn moments each occur in a parallel and antiparallel orientation thus generating six magnetic sublattices. The non-collinearity is attributed to anisotropy and frustration. In the AF1 phase, the crystal structure can be described with orthorhombic symmetry without inversion symmetry. Both transitions have been suggested to be of first order[23,24]. Elastic neutron-scattering experiments have shown that the magnetic texture of the non-collinear AF1 phase strongly changes in an applied magnetic field[19,21]. In light of the decisive effect of magnetic texture on the Berry curvature this feature is exactly what is needed to generate large variations of the Hall effect in increasing magnetic field.

Results

Figure 1 shows Hall-effect measurements in the non-collinear phase of Mn$_5$Si$_3$ single crystals with different orientations of the applied magnetic field H with respect to the crystallographic axes. We observe multiple transitions with sign changes of ρ_{yx} and a strong anisotropy of the AHE, in particular when comparing the cases for $H\|c$ (Fig. 1a) and $H\|a$ (Fig. 1c). In addition to the jump and a hysteresis of ρ_{yx} around zero field, Fig. 1a shows two jumps of ρ_{yx} at higher fields in positive and negative field direction. The jump at zero field is absent for field orientations along the orthorhombic b and a axes (Fig. 1b,c). At fields above 5 T at $T = 50\,K$, the Hall effect almost vanishes for all field orientations. While the H direction plays a distinctive role as just discussed, the perpendicular relative orientations of current direction and voltage drop do not entail large differences, cf. upper and lower panels in Fig. 1a–c.
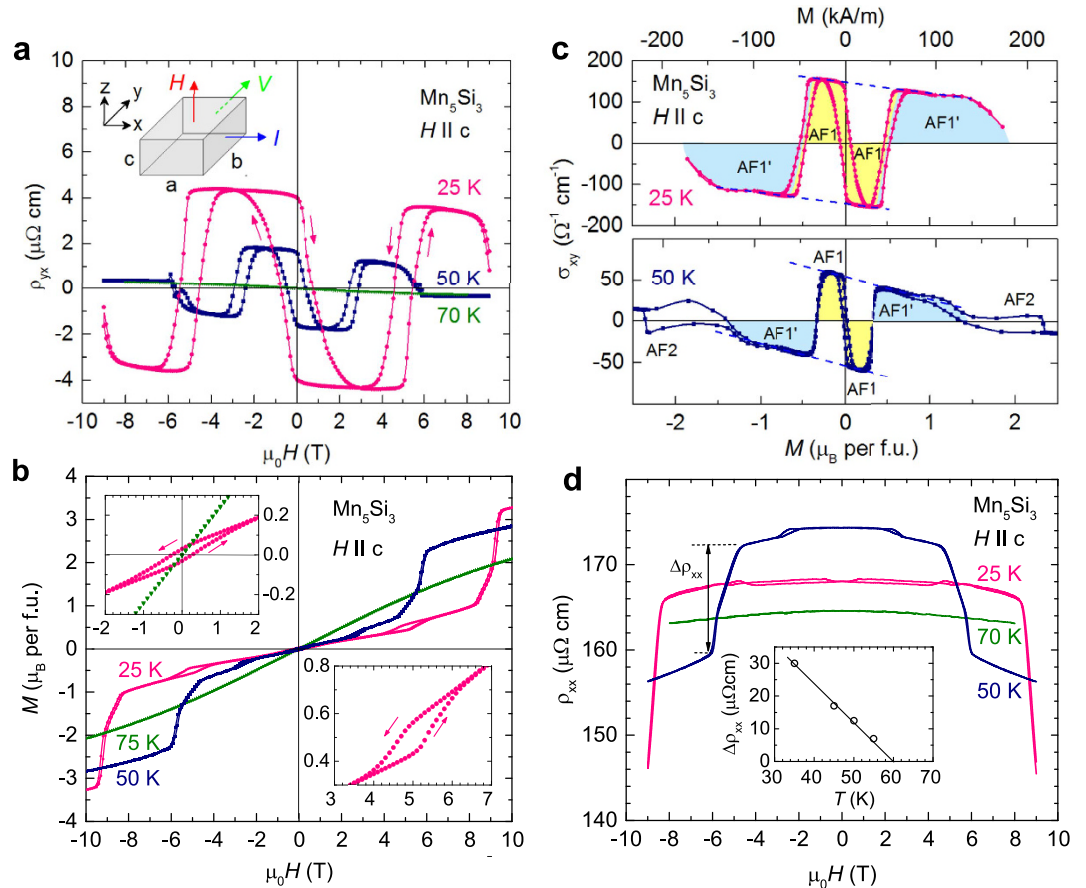
Figure 2. Anomalous Hall effect for *H* along *c* and current *I* along *a*. (**a**) Hall resistivity $\rho_{yx}(H)$ at $T = 25$ K and 50 K (below $T_{N1} = 60$ K) and at $T = 70$ K between T_{N1} and T_{N2}. (**b**) Magnetization $M(H)$ for $T = 25$, 50, and 75 K. Insets show $M(H)$ in a small range of H. (**c**) Hall conductivity σ_{xy} vs. magnetization M. Blue broken lines indicate a linear behaviour of σ_{xy} observed in restricted regions of M. Coloured areas indicate the two non-collinear magnetic phases. (**d**) Magnetoresistivity $\rho_{xx}(H)$. Inset shows the temperature dependence of the jump $\Delta\rho_{xx}$ at the metamagnetic transition.

In the following we will focus on the results for the orientation $H\|c$, for which a large spontaneous Hall effect at zero field, a second transition at intermediate fields, and a third transition at high fields is observed. (The behaviour of ρ_{yx} with the field oriented along the b axis has been reported previously[18]. Figure 2a shows that for the field direction $\|c$, the Hall effect decreases with increasing temperature and vanishes above $T_{N1} \approx 60$ K. While ρ_{yx} at 25 K has two remanent states at $\pm 4\,\mu\Omega$cm at zero field, the magnetization shows only a weak difference of $M(0) = \pm 0.03\,\mu_B$/f.u. in the hysteresis at zero field (Fig. 2b, upper left inset). This difference arises from a reorientation of weakly ferromagnetically coupled Mn_1 moments inferred from the magnetic susceptibility of Mn_5Si_3 polycrystals, suggesting a magnetic-field induced second-order transition[25]. However, from the hysteresis of M and ρ_{xy} around zero field it appears more likely that a first-order transition occurs due to a "switching" of Mn_1 moments in a weak field which gives rise to shallow variations of M but huge contributions to the AHE.

At the second transition around 5 T at 25 K, ρ_{yx} switches back by the same amplitude as at zero field, whereas the corresponding change of magnetization $M(0) = \pm 0.06\,\mu_B$/f.u. (Fig. 2b, lower left inset) is a factor two larger than at zero field. This transition is accompanied by a 1-% volume compression of the crystal lattice and has been attributed to a field-induced magnetostructural modification of the AF1 phase[21,22]. Here, the magnetic field perturbs the weak ferromagnetic coupling between neighbouring Mn_1 moments arranged in chains along the crystallographic c axis. The order of the Mn_1 moments is lost but the Mn_2 moments are still arranged in a non-collinear fashion[22]. This magnetic phase is labeled AF1'. At 58 K, an aligned moment of $\approx 0.18\,\mu_B$/Mn has been observed by neutron scattering[21]. In the present case, the jump observed at $\approx \pm 3$ T and 50 K corresponds to an increase of M by $0.06\,\mu_B$/Mn.

The dependence of the Hall conductivity σ_{xy} on the magnetization M is shown in Fig. 2c, where the coloured areas indicate the different magnetic phases. Apart from the distinct hysteretic transitions, the Hall conductivity follows a linear behaviour $\sigma_{xy} = -0.032\,V^{-1}M$ with the same slope being observed at 25 K and 50 K, see blue broken lines in Fig. 2c. The linear behaviour corresponds to the roughly linearly increasing background magnetization $M(H)$ observed in the AF2 phase at $T = 75$ K (Fig. 2c) and attributed to a tilting of Mn_2 moments in magnetic field. No hysteretic transitions have been observed above T_{N1}. The $\sigma_{xy}(M)$ data at 75 K have been
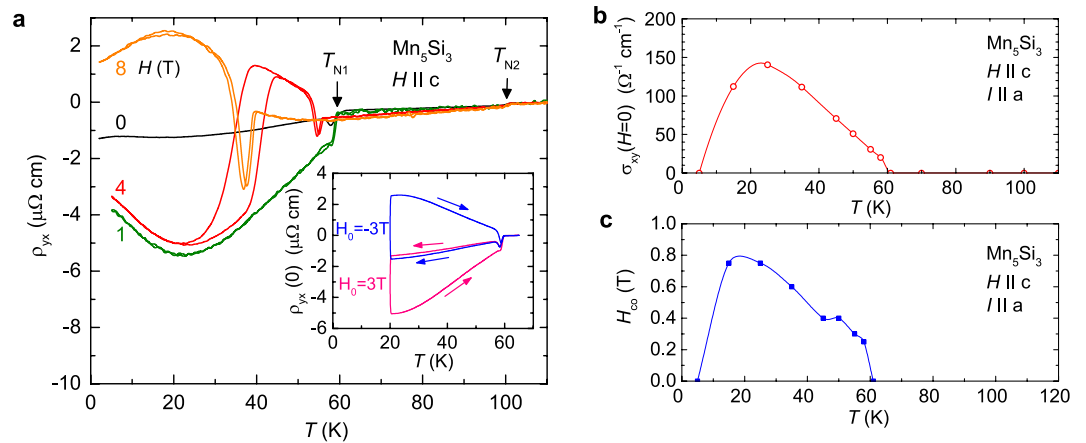
Figure 3. Temperature dependences. (**a**) Temperature dependence of the Hall resistivity ρ_{yx} in different magnetic fields. Inset shows the temperature dependence of the remanent AHE $\rho_{yx}(H=0)$ after a magnetic field of $+3\,T$ or $-3\,T$ was switched on and off at $T=20\,K$. (**b**) Hall conductivity at zero field $\sigma_{xy}(0) \approx \rho_{yx}(0)/\rho_{xx}^2$. (**c**) The coercive field H_{co} of the Hall resistivity around zero field.

used to disentangle the contributions arising from the ordinary Hall effect and from the AHE[17]. We obtain $R_0 = 6 \times 10^{-10}\,m^3/As$ and $S_H = -0.0173\,V^{-1}$ at 75 K in agreement with values obtained for polycrystalline Mn_5Si_3 films[17].

The jump of ρ_{yx} back to the smooth 70-K curve occurs at ± 5 and $\pm 9\,T$ for $T=25\,K$ and 50 K, respectively (Fig. 2a). This third transition is accompanied by a strong increase of M by $\approx 2.1(1.3)\,\mu_B/f.u.$ at 25 (50) K (Fig. 2b) due to a first-order metamagnetic transition arising from a rearrangement of Mn_2 moments to a magnetic state akin to the collinear AF2 phase[25,26]. The same behaviour is observed in the reverse field direction thus leading to distinct transitions of the Hall effect at the metamagnetic transitions AF1 → AF1' and AF1' → AF2 for each magnetic field direction. At high fields, i.e., above these transitions, the $\rho_{yx}(H)$ data for $T=50\,K$ and $T=70\,K$ coincide, indicating similarity of magnetic structure and/or Berry curvature.

A strong field dependence is also observed in the magnetoresistivity $\rho_{xx}(H)$, see Fig. 2d. $\rho_{xx}(H)$ shows minor variations at low fields but a huge jump towards lower resistivity corresponding to a magnetoresistance ratio (MR) $\rho_{xx}(H)/\rho_{xx}(0) = 17\%$, and an almost linear decrease towards higher fields, see the data for $T=50\,K$ in Fig. 2d. The jump disappears at T_{N1}, see inset Fig. 2d.

The fact that the AHE vanishes in the collinear AF2 phase at temperatures $T > T_{N1}$ or at high fields suggests that all variations of ρ_{yx} or σ_{xy} and $M(H)$ below the high-field transition to the AF2 phase occur between two non-collinear magnetic phases AF1 and AF1' with different magnetic-moment arrangements leading to sign changes of the AHE of similar size. Hence, a full reversal of the Hall effect is observed when the magnetic structure changes between two non-collinear states by application of a magnetic field.

The evolution of the AHE in the different magnetic states is also seen in the temperature dependence of the Hall effect at different applied magnetic fields, Fig. 3a. A strong variation of ρ_{yx} is observed for $T < T_{N1}$. With decreasing temperature, $\rho_{yx}(T)$ either decreases in a low field (1 T), or first increases and then decreases at intermediate field (4 T), or increases steadily for high field (8 T). The pronounced dips are artefacts due to misaligned contacts leading to a contribution from $\rho_{xx}(T)$ to $\rho_{yx}(T)$ which is considerably large at the metamagnetic transition, cf. Fig. 2d. The offset was roughly compensated in the paramagnetic state at $T=110\,K$, see Supplementary Information, but could not be completely reduced during the temperature-dependent measurement. Figure 3a (inset) shows that after zero-field cooling to 20 K and switching the magnetic field on and subsequently off in either direction generates a remanent AHE which decreases with increasing temperature to zero at T_{N2}. The maximum of $\sigma_{xy}(H=0) = 140\,\Omega^{-1}cm^{-1}$ at $T=25\,K$ corresponds to an apparent AHE coefficient $S_H^0 = \sigma_{xy}/M = -5.1\,V^{-1}$ in zero field, very similar to values observed for the non-collinear antiferromagnets Mn_3Sn ($S_H^0 = -8.3\,V^{-1}$)[3] and Mn_3Ge ($S_H^0 = -1.3\,V^{-1}$)[2]. S_H^0 is much larger than the slope of $\sigma_{xy}(M)$ arising form the background magnetization in the AF1 phase, see the blue broken lines in Fig. 2c.

At temperatures below 20 K, the magnitude of the AHE decreases again. This is possibly due to a further change of the magnetic structure of Mn_5Si_3 at low temperatures which has not been investigated in detail up to now. In Mn_5Si_3 polycrystals, a small change of the magnetic susceptibility at $T=30\,K$ was tentatively interpreted as being associated with a rearrangement of weakly coupled spins in the magnetically frustrated configuration[22]. A similar temperature dependence is observed for the zero-field Hall conductivity $\sigma_{xy}(H=0)$ (Fig. 3b) and the corresponding coercive field H_{co} (Fig. 3c).

From the transitions observed in ρ_{yx}, $M(H)$, and ρ_{xx} (see Supplementary Information), we obtain the magnetic phase diagram for Mn_5Si_3, Fig. 4. T_{N1} decreases strongly with increasing field while T_{N2} does not change with field. Below $T_{N1} = 60\,K$, a new intermediate phase AF1' between the non-collinear phase AF1 and the collinear phase AF2 is established. This phase must also host a non-collinear magnetic structure because ρ_{yx} is nonzero in this regime and $\rho_{yx} = 0$ in the collinear phase. The state above T_{N1} or in high magnetic fields is thought to be akin to the collinear AF2 phase at $T > 60\,K$ due to the similar behaviour of $\rho_{yx}(H)$, see Fig. 2a for $T=50\,K$ and 70 K.
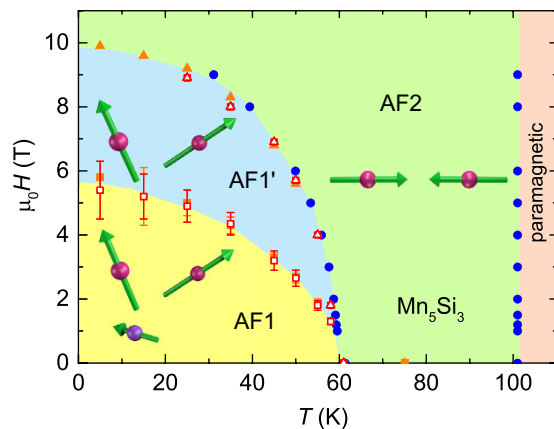
Figure 4. Magnetic phase diagram of Mn$_5$Si$_3$. Data obtained from measurements of Hall effect (red open symbols), resistivity (blue dots), and magnetization (orange triangles). Error bars indicate the hysteresis width of $\rho_{yx}(H)$. Arrows visualize the relative non-coplanar orientations between Mn$_1$ moments (violet) and Mn$_2$ moments (red) in the AF1 and AF1' phases. The second set of antiparallel oriented moments is not shown.
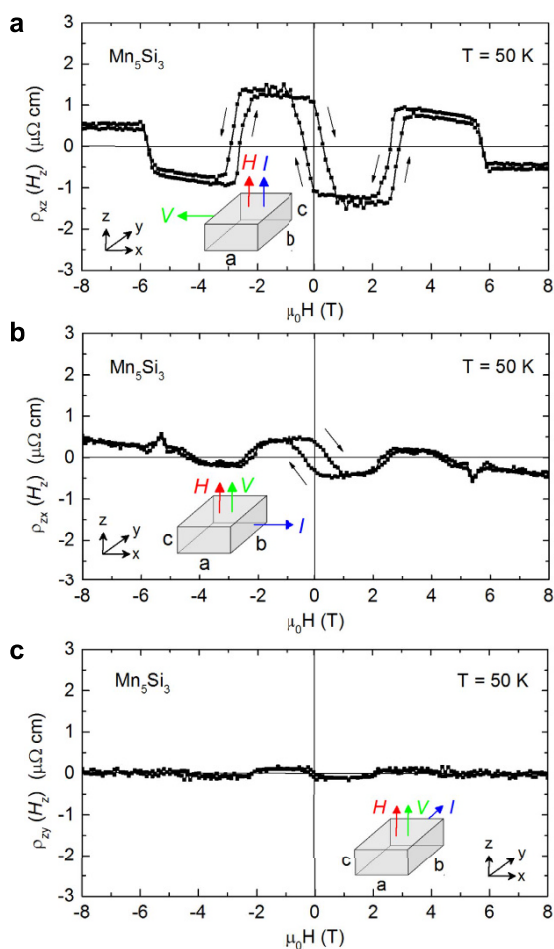

Figure 5. Unusual Hall effects of Mn$_5$Si$_3$ below T$_{N1}$ = 60 K. Hall resistivities $\rho_{\alpha\beta}(H_z) = V_\alpha/I_\beta$ where either the current I or the voltage V transverse to the current is parallel to the magnetic field oriented along the crystallographic c axis. (**a**) Longitudinal Hall effect. (**b,c**) Unconventional Hall effect.

In addition to the conventional Hall effect, where current, voltage, and magnetic field are mutually oriented perpendicularly, we observe strong voltages transverse to the current when either the current, i.e., electrical field, or the voltage is oriented parallel to the magnetic field along the crystallographic c axis (Fig. 5a and b

respectively). These unusual configurations are assigned as "longitudinal" or "unconventional" Hall effects, respectively[27]. The former is related to the so-called "planar Hall effect" which is usually maximal at an angle of 45° between the magnetic field and current direction and arises from the anisotropic magnetoresistance. The unconventional Hall effect, on the other hand, has to be attributed to effects arising from the Berry curvature. We note that in Mn_5Si_3 the unconventional Hall effect with the voltage perpendicular to the current but parallel to H is only minor (Fig. 5c). Such unconventional Hall effects have been reported for Weyl semi-metals where anomalous magnetotransport phenomena (Adler-Bell-Jackiw anomaly) are observed due to a "topological" $E \cdot B$ term in the presence of weak antilocalization[27]. The existence of Weyl points or avoided crossings that develop in the electronic structure close to the Fermi level has also been suggested for the half-Heusler antiferromagnet GdPtBi exhibiting a large AHE[1]. However, the observed strong unconventional Hall effect in Mn_5Si_3 could alternatively arise from the strong anisotropy of the magnetic structure and AHE, cf. Fig. 1. A full quantitative explanation of the size and sign of the AHE in Mn_5Si_3 with the hitherto unique feature of a sequence of non-collinear phases must await electronic band-structure calculations to obtain the Berry curvature and magnon dispersion in the different magnetic phases. This is challenging due to the magnetic superstructure in the non-collinear regime.

Discussion

We have observed multiple transitions of the Hall effect, each within a narrow field region. The data clearly demonstrate that the Berry curvature and, hence, the AHE are very sensitive to a field-induced switching of the spin-texture phase even though the magnetization shows only shallow variations due to partly compensated moments in the non-collinear antiferromagnetic phase. Magnetic-field-induced transitions between multiple magnetic phases are typically observed in magnetically frustrated systems, where the frustration arises either from the geometry of the crystal lattice or from competing interactions between magnetic moments[28]. The example of Mn_5Si_3, where the non-collinear magnetic order is due to anisotropy and frustration, suggests that a number of similar metallic compounds with complex magnetic structures possibly exhibit large variations of the Hall response in magnetic field which makes such materials attractive for applications relying on magnetic-field induced switching of electronic transport properties.

Methods

The Mn_5Si_3 single crystals were obtained by a combined Bridgman and flux-growth technique using a Mn-rich self flux and a low cooling rate of 1.2 °C/h. The crystals were characterized by powder x-ray diffraction, confirming the formation of the Mn_5Si_3 phase. Three cuboid pieces of mm- to sub-mm length and thickness with different orientations of the crystallographic a_h and c_h axes with respect to the sample edges were obtained after Laue diffraction. Resistivity and Hall-effect measurements were performed in a physical-property measurement system (PPMS) with the field oriented along the z direction perpendicular to the sample xy plane. 120-μm Cu wires were attached to the crystal with conductive silver-epoxy (EPOTEK H20E). Each sample was mounted in different orientations with respect to the magnetic field direction. Data were taken for both field directions and were symmetrized, see Supplementary Information. Due to the different contact configurations, i.e., separation of the Hall-voltage contacts, some data exhibit a slightly stronger scatter compared to other, cf. upper and lower panels of Fig. 1. Magnetization curves were acquired in a vibrating sample magnetometer (VSM) up to 12 T and in a SQUID magnetometer up to 5 T with the field applied in the same orientation as for the Hall-effect measurements.

References

1. Suzuki, T. et al. Large anomalous Hall effect in a half-Heusler antiferromagnet. Nat. Phys. **12,** 1119–1123 (2016).
2. Nayak, A. K. et al. Large anomalous Hall effect driven by a nonvanishing Berry curvature in the non-collinear antiferromagnet Mn_3Ge. Sci. Adv. **2,** e1501870; doi: 10.1126/sciadv.1501870 (2016).
3. Nakatsuji, S., Kiyohara, N. & Higo, T. Large anomalous Hall effect in a non-collinear antiferromagnet at room temperature. Nature **527,** 212–215 (2015).
4. Gomonay, O. Berry-phase effects and electronic dynamics in a noncollinear antiferromagnetic texture. Phys. Rev. B **91,** 144421 (2015).
5. Chen, H., Niu, Q. & MacDonald, A. H. Anomalous Hall effect arising from noncollinear antiferromagnetism. Phys. Rev. Lett. **112,** 017205 (2014).
6. Shindou, R. & Nagaosa, N. Orbital ferromagnetism and anomalous Hall effect in antiferromagnets on the distorted fcc lattice. Phys. Rev. Lett. **87,** 116801 (2001).
7. Nagaosa, N., Sinova, J., Onoda, S., MacDonald, A. H. & Ong, N. P. Anomalous Hall effect. Rev. Mod. Phys. **82,** 1539–1592 (2010).
8. Xiao, D., Chang, M.-C. & Niu, Q. Berry phase effects on electronic properties. Rev. Mod. Phys. **82,** 1959–2007 (2010).
9. Machida, Y., Nakatsuji, S., Onoda, S., Tayama, T. & Sakakibara, T. Time-reversal symmetry breaking and spontaneous Hall effect without magnetic dipole order. Nature **463,** 210–213 (2010).
10. Schulz, T. et al. Emergent electrodynamics of skyrmions in a chiral magnet. Nat. Phys. **8,** 301–304 (2012).
11. Ueland, B. G. et al. Controllable chirality-induced geometrical Hall effect in a frustrated highly correlated metal. Nat. Commun. **3,** 1067, doi: 10.1038/ncomms2075 (2012).
12. Nagaosa, N. & Tokura, Y. Topological properties and dynamics of magnetic skyrmions. Nat. Nanotechnol. **8,** 899–911 (2013).
13. Jungwirth, T., Marti, X., Wadley, P. & Wunderlich, J. Antiferromagnetic spintronics. Nat. Nanotechnol. **11,** 231–241 (2016).
14. Baltz, V. et al. Antiferromagnetism: the next flagship magnetic order for spintronics? arXiv:1606.04284 [cond-mat] (2016).
15. MacDonald, A. H. & Tsoi, M. Antiferromagnetic metal spintronics. Phil. Trans. R. Soc. A **369,** 3098–3114 (2011).
16. Cheng, R., Xiao, J., Niu, Q. & Brataas, A. Spin Pumping and Spin-Transfer Torques in Antiferromagnets. Phys. Rev. Lett. **113,** 057601 (2014).
17. Sürgers, C., Fischer, G., Winkel, P. & Löhneysen, H. v. Large topological Hall effect in the non-collinear phase of an antiferromagnet. Nat. Commun. **5** 3400, doi: 10.1038/ncomms4400 (2014).
18. Sürgers, C., Kittler, W., Wolf, T. & Löhneysen, H. v. Anomalous Hall effect in the noncollinear antiferromagnet Mn_5Si_3. AIP Advances **6,** 055604, doi: 10.1063/1.4943759 (2016).
19. Brown, P. J., Forsyth, J. B., Nunez, V. & Tasset, F. The low-temperature antiferromagnetic structure of Mn_5Si_3 revised in the light of neutron polarimetry. J. Phys.: Condens. Matter **4,** 10025 (1992).

20. Brown, P. J. & Forsyth, J. B. Antiferromagnetism in Mn$_5$Si$_3$: the magnetic structure of the AF2 phase at 70 K. *J. Phys.: Condens. Matter* **7,** 7619 (1995).
21. Silva, M. R., Brown, P. J. & Forsyth, J. B. Magnetic moments and magnetic site susceptibilities in Mn$_5$Si$_3$. *J. Phys.: Condens. Matter* **14,** 8707 (2002).
22. Gottschilch, M. *et al.* Study of the antiferromagnetism of Mn$_5$Si$_3$: an inverse magnetocaloric effect material. *J. Mater. Chem.* **22,** 15275–15284 (2012).
23. Barmin, S. M., Mikhel'son, A. V., Sevast'yanov, A. A., Kortov, S. V. & Gel'd, P. V. Thermal expansion of Mn$_5$Si$_3$ single crystals. *Sov. Phys. Solid State* **26,** 1977 (1984).
24. Vinokurova, L., Ivanov, V. & Kulatov, E. Magnetic phase transitions in single crystals of Mn$_5$Si$_3$ and (Mn,Fe)$_5$Si$_3$. *Physica B: Condensed Matter* **211,** 96–98 (1995).
25. Al-Kanani, H. J. & Booth, J. G. Magnetic field induced transitions in Mn$_5$Si$_3$. *J. Magn. Magn. Mater.* **140–144,** 1539–1540 (1995).
26. Vinokurova, L., Ivanov, V., Kulatov, E. & Vlasov, A. Magnetic phase transitions and electronic structure of the manganese silicides. *J. Magn. Magn. Mater.* **90 & 91,** 121–125 (1990).
27. Kim, H.-J. *et al.* Dirac versus Weyl fermions in topological insulators: Adler-Bell-Jackiw anomaly in transport phenomena. *Phys. Rev. Lett.* **111,** 246603 (2013).
28. Kawamura, H. Universality of phase transitions of frustrated antiferromagnets. *J. Phys.: Condens. Matter* **10,** 4707 (1998).

Acknowledgements

Author Contributions

C.S. conducted the electronic-transport measurements, T.W. grew the single crystals, P.A. performed the x-ray characterization, W.K. and G.F. conducted the magnetization measurements, C.S. and H.v.L. wrote the main manuscript text. All authors reviewed the manuscript.

Additional Information

Supplementary information accompanies this paper at http://www.nature.com/srep

Competing financial interests: The authors declare no competing financial interests.

How to cite this article: Sürgers, C. *et al.* Switching of a large anomalous Hall effect between metamagnetic phases of a non-collinear antiferromagnet. *Sci. Rep.* **7,** 42982; doi: 10.1038/srep42982 (2017).

Publisher's note: Springer Nature remains neutral with regard to jurisdictional claims in published maps and institutional affiliations.